



Contents lists available at ScienceDirect

Quaternary Science Reviews

journal homepage: www.elsevier.com/locate/quascirev

Beach ridges as paleoseismic indicators of abrupt coastal subsidence during subduction zone earthquakes, and implications for Alaska-Aleutian subduction zone paleoseismology, southeast coast of the Kenai Peninsula, Alaska

Harvey M. Kelsey^{a,*}, Robert C. Witter^b, Simon E. Engelhart^c, Richard Briggs^d, Alan Nelson^d, Peter Haeussler^b, D.Reide Corbett^e

^a Department of Geology, Humboldt State University, Arcata, CA 95524, USA

^b U. S. Geological Survey, Alaska Science Center, 4210 University Drive, Anchorage, AK 99508, USA

^c Department of Geosciences, University of Rhode Island, 9 E. Alumni Ave., Kingston, RI 02881, USA

^d Geologic Hazards Team, US Geological Survey, Golden, CO 80225, USA

^e Department of Geological Sciences, East Carolina University, Greenville, NC 27858, USA

ARTICLE INFO

Article history:

Received 2 June 2014

Received in revised form

17 December 2014

Accepted 8 January 2015

Available online xxx

Keywords:

Paleoseismology

Subduction zone earthquakes

Alaska-Aleutian subduction zone

Kenai Peninsula

Beach ridges

Subduction zone segments

Subduction zone

ABSTRACT

The Kenai section of the eastern Alaska-Aleutian subduction zone straddles two areas of high slip in the 1964 great Alaska earthquake and is the least studied of the three megathrust segments (Kodiak, Kenai, Prince William Sound) that ruptured in 1964. Investigation of two coastal sites in the eastern part of the Kenai segment, on the southeast coast of the Kenai Peninsula, identified evidence for two subduction zone earthquakes that predate the 1964 earthquake. Both coastal sites provide paleoseismic data through inferred coseismic subsidence of wetlands and associated subsidence-induced erosion of beach ridges. At Verdant Cove, paleo-beach ridges record the paleoseismic history; whereas at Quicksand Cove, buried soils in drowned coastal wetlands are the primary indicators of paleoearthquake occurrence and age. The timing of submergence and death of trees mark the oldest earthquake at Verdant Cove that is consistent with the age of a well documented ~900-year-ago subduction zone earthquake that ruptured the Prince William Sound segment of the megathrust to the east and the Kodiak segment to the west. Soils buried within the last 400–450 years mark the penultimate earthquake on the southeast coast of the Kenai Peninsula. The penultimate earthquake probably occurred before AD 1840 from its absence in Russian historical accounts. The penultimate subduction zone earthquake on the Kenai segment did not rupture in conjunction with the Prince William Sound to the northeast. Therefore the Kenai segment, which is presently creeping, can rupture independently of the adjacent Prince William Sound segment that is presently locked.

© 2015 Elsevier Ltd. All rights reserved.

1. Introduction

1.1. Tectonic context of the investigation

In March 1964, an 800-km-long rupture of the eastern Alaska-Aleutian megathrust (Plafker, 1969) (Fig. 1A) involved along-strike variations in coseismic slip that define separate segments of the megathrust (Christensen and Beck, 1994). Megathrust slip was

highest (up to 20 m) on the Prince William Sound (PWS) and Kodiak segments, and less on the Kenai segment (Suito and Freymueller, 2009). These segments also show contemporary along-strike variability in interplate coupling derived from GPS velocities in the region of the 1964 rupture (Freymueller et al., 2008). GPS observations indicate that presently the PWS and Kodiak segments of the megathrust are locked and the Kenai segment is creeping (Fig. 1A).

The Kenai segment, between the Kodiak and PWS segments of the Alaskan megathrust (Fig. 1A), has an unknown earthquake history prior to 1964. Plafker (1969) identified coastal forests drowned after the 1964 earthquake and measured vertical shifts of

* Corresponding author. Tel.: +1 707 543 6763.

E-mail address: hmk1@humboldt.edu (H.M. Kelsey).

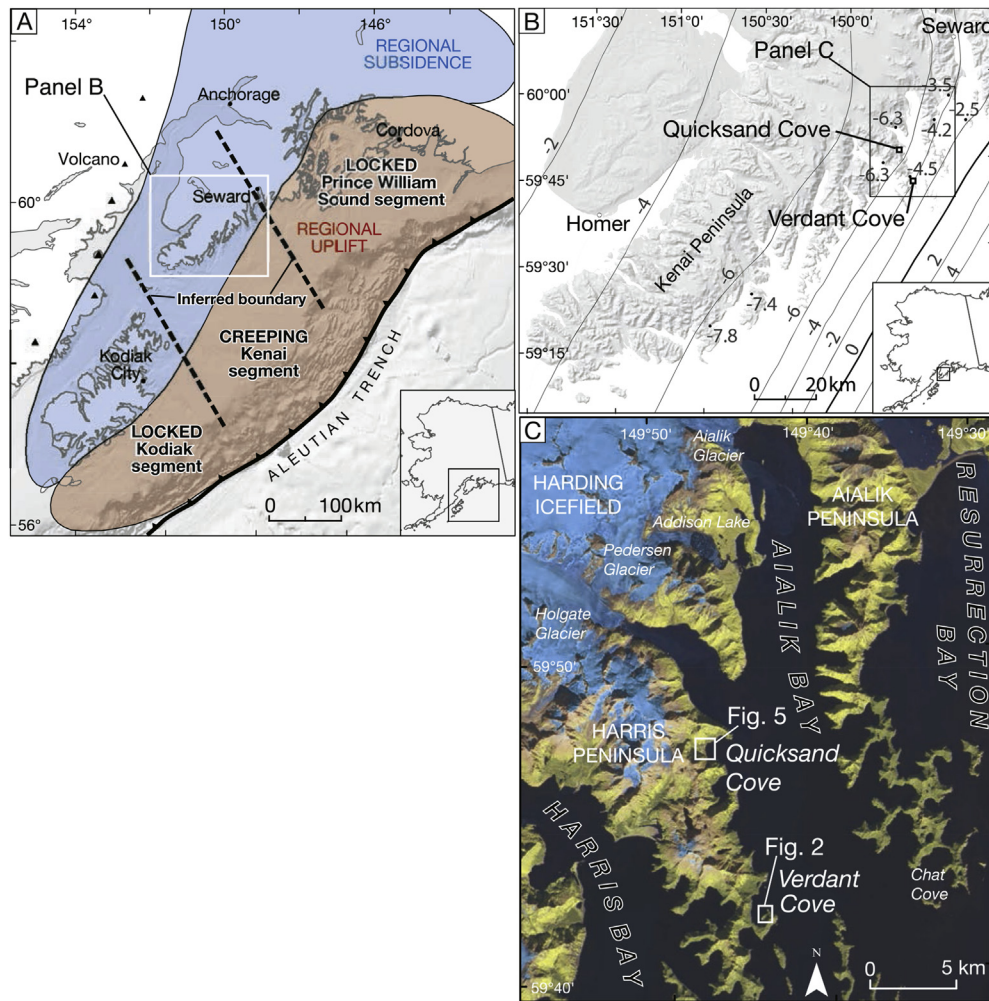


Fig. 1. A. Tectonic setting of the eastern Alaska-Aleutian subduction zone megathrust. Bold line delineates the surface trace of the megathrust, barbs on upper (North American) plate. Vertical deformation during the 1964 great Alaska earthquake depicted by two adjoining margin-parallel belts: a region of landward subsidence (blue) and a region of seaward uplift (red) (Plafker, 1969). Areas of highest slip occurred below the Prince William Sound and Kodiak segments, which are currently locked currently; while the intervening Kenai segment is creeping presently (Freymueller et al., 2008). B. Map of the Kenai Peninsula that shows contours of vertical deformation, in feet, caused by the 1964 Alaska earthquake (Plafker, 1969). Black circles mark sites where subsidence in 1964 was reported by Plafker (1969). Black open squares, two field sites; note that Quicksand Cove site is in the axis of maximum subsidence as a result of the 1964 subduction zone earthquake. C. Landsat image from 4 May 2014 showing the two paleoseismic sites within Kenai Fjords National Park. The white dashed line to the west and northwest of Quicksand Cove is the outline of the basin that drains into the Quicksand Cove coastal wetland.

the shoreline indicative of tectonic subsidence along the south-eastern Kenai Peninsula (Fig. 1A and B), but reported no evidence of older Holocene earthquakes. Mann and Crowell (1996) reported ghost forests killed by the 1964 earthquake at several sites on the southeast Kenai coast and evidence for an earlier earthquake about 900 years ago at Verdant Cove. Carver and Plafker (2008) summarize evidence for nine prehistoric earthquakes in the Prince William Sound region inferred from geological evidence for sudden land-level change and, in some cases, tsunami deposits. Radiocarbon-based earthquake chronologies suggest the most recent predecessor to the 1964 earthquake in the Prince William Sound area occurred about 900 years ago and time intervals between earthquakes ranged from around 390 to 900 years (Carver and Plafker, 2008; Shennan et al., 2014a, 2014b). By contrast, paleoseismic evidence to the west of the Kenai Peninsula, at Sitkinak and Kodiak Islands, imply a different earthquake history. Sites on both islands suggest that in addition to a great earthquake about 900 years ago, a historic earthquake ruptured near Sitkinak and Kodiak in AD 1788 (Briggs et al., 2014; Shennan et al., 2014c) and another large or great earthquake occurred between AD 1430 to AD 1650 (Briggs et al., 2014; Shennan et al., 2014a, 2014c).

1.2. Statement of the problem

Our investigations sought evidence for Aleutian megathrust earthquakes and tsunamis, including the 1964 earthquake, in the boundary region between the Kenai and PWS segments (Fig. 1). The problem we address is that, although in 1964 the Aleutian megathrust ruptured from Prince William Sound to the southwest end of Kodiak segment (Plafker, 1969), rupturing through what is now the central creeping Kenai segment, the history of earlier subduction zone earthquakes in the Kenai segment is unknown. To address the problem, we reconstructed a record of prehistoric earthquakes and tsunamis along the Kenai segment to compare with paleoseismic records from the PWS and Kodiak segments.

To investigate tectonic history of the Kenai segment of the subduction zone, we focus field work on the southeast Kenai coast where there was >1 m of coseismic subsidence during the 1964 earthquake (Fig. 1B); and where the coastal setting has a high potential for preservation of a record of earlier instances of subsidence. The southeast Kenai coast is a high-wave-energy coast that receives sediment from basins that were extensively glaciated at the Last Glacial Maximum and glaciated to a lesser extent during

the glacial re-advance of the Little Ice Age (Fig. 1C). The abundant sediment supply from Kenai Mountains combined with the high-wave-energy environment makes for coastal settings that challenge traditional coring methods employed in lower-wave-energy coasts that drain unglaciated basins (e. g., Witter et al., 2003). Therefore, the scientific problem is to ascertain, within a high-wave-energy and high-sediment-discharging coastal environment, if evidence for subduction zone earthquakes is formed and preserved in coastal sediments.

1.3. Research objectives

The research objectives of this paper are threefold. First, we describe two sites on the southeast Kenai coast that provide a paleoseismic record of subduction zone earthquakes (Verdant Cove and Quicksand Cove, Fig. 1C). Second, we discuss number and age of paleoearthquakes inferred at the two sites, justify these inferences and then explore any likely correlation of the earthquake history to paleoseismic histories at locations on the subduction zone along strike to the northeast and the southwest. Third, we address the question: Under what condition can a sequence of beach ridges record the effects of subduction zone earthquakes?

2. Research approach and methods

The two field sites on the southeast coast of the Kenai Peninsula were selected using satellite and conventional aerial photographic imagery. The selection process entailed evaluating over thirty candidate wetlands on the southeast Kenai coast, subsequently visiting six of these wetlands in the field, and selecting two sites that directly address the research objectives. For each site, the field goal was to collect data that would inform the late Holocene geomorphic and sedimentation history. To this end, field data included stratigraphy as observed in cutbank outcrops and cores, locations determined with a hand-held Global Positioning System (GPS) unit, elevation profile data collected with a real-time kinematic (RTK) GPS unit and sediment samples for chronostratigraphic, microfossil and grain size analyses. Determinations of subsurface stratigraphy utilized gouge corers (2.5 cm diameter) and both a Russian peat auger and a fat gouge corer for larger diameter (5 cm) samples.

Radiocarbon samples came from detrital organic fragments within the uppermost one to two cm of a buried soil or directly above the buried soil. Sample material avoided charcoal fragments and only seeds and small (<3 mm diameter) twigs with branching nodes were considered suitable for analysis. Radiocarbon sample material was extracted from a 1 mm sieve, picked clean of modern roots and sediment, washed with distilled water, air dried and submitted for analysis. Radiocarbon AMS ages were determined by NOSAMS and then calibrated using Oxcal version 4.2.3. (Bronk Ramsey, 2009) and the IntCal2013 dataset (Reimer et al., 2013). All calibrated ages are reported as age ranges at two standard deviations in cal yr BP (BP, before present), where present is AD 1950. ^{210}Pb , ^{226}Ra , ^{137}Cs , and ^{40}K activities were determined by gamma spectroscopy on low-background, high-efficiency, high-purity Germanium detectors. The goal was to identify the ^{137}Cs peak (AD 1963) activity. ^{210}Pb -based sediment accumulation rates were not calculated because of abrupt sedimentological changes associated with a subduction zone setting where both soil submergence and tsunami deposition are common. Samples were initially dried, homogenized by grinding, packed into standardized vessels, and sealed for at least 24 h before counting. Activities were corrected for self-absorption using a direct transmission method (Cutshall et al., 1983; Cable et al., 2001). Excess ^{210}Pb activities were determined by subtracting total ^{210}Pb from that supported by ^{226}Ra , determined

indirectly by counting the gamma emissions of its granddaughters, ^{214}Pb and ^{214}Bi .

3. Previous work at verdant cove

In the course of archeological reconnaissance on the Verdant Cove coastal plain (Fig. 1C), Mann and Crowell (1996) divided the coastal plain into two surfaces, the lower elevation *Elymus* surface and the higher elevation *Tsuga* surface. They constructed a level-line topographic profile that depicts the two surfaces as well as a tidal pond situated between the *Tsuga* surface and the base of the upland.

At low tide, the tidal pond exposed in-growth-position buried tree trunks (Mann and Crowell, 1996). Mann and Crowell (1996) obtained radiocarbon ages for these stumps (Table 1), inferred that the stumps were killed by coseismic subsidence and further inferred that subsidence occurred during a ca 900 year earthquake on the Aleutian subduction zone.

4. Results

4.1. Overview of coastal sites

Multiple beach ridges are characteristic of both sites. Beach ridges (including “storm berms”) are wave-swash-created features that, if separated from the active beach by relative sea-level fall, or by coastal progradation, can be sea level indicators (Wells, 1996; Otvos, 2000; Goy et al., 2003; Hein et al., 2013). For the two coastal sites (Fig. 1C), a combination of coastal plain stratigraphy and observations on the generation and modification of beach ridges provide data to address late Holocene relative sea level changes and subduction zone paleoseismic history. The two sites are within 10 km of each other, and therefore experienced the same subduction zone earthquakes and approximately the same amount of coseismic land level change during these earthquakes.

4.2. Verdant Cove

The Verdant Cove composite strand plain (a strand plain is a broad plain of sand along a shoreline exhibiting parallel or semi-parallel sand ridges separated by shallow swales (e. g., Goy et al., 2003)) is composed of three beach ridge sets with each set having an erosional escarpment on its seaward side. The three beach ridge sets (‘oceanward’, ‘middle’ and ‘landward’, Fig. 2) are progressively younger to the northwest. On the level-line topographic profile constructed across the Verdant Cove progradational plain by Mann and Crowell (1996), the topographic expression of the three beach ridge sets is apparent (Fig. 3). The topographic profile shows that the crest of seaward-most beach ridge of each beach ridge set gets higher in a northwestward (coastward) direction.

Mann and Crowell (1996) mapped two surfaces on the Verdant Cove composite strand plain, and these surfaces are the same features that we map as sets of beach ridges (Fig. 2). However, Mann and Crowell’s (1996) upper surface includes both the middle and landward set of beach ridges (Fig. 2) because they did not recognize the middle beach ridge set. The middle beach ridge set is clearly defined by bounding paleo beach escarpments as well as by a depression at its landward edge (Fig. 2).

The three beach ridge sets share similar morphology. Each beach ridge set is fronted on its oceanward side by a 1-m to 3-m high beach ridge that parallels the modern coastline. The frontal beach ridge has a prominent escarpment on the seaward side. Behind each of these frontal beach ridges (i.e. to the southeast) is a strand plain (Fig. 3). Each strand plain represents gradual westward

Table 1

Radiocarbon age estimates for samples from Quicksand Cove and Verdant Cove, Aialik Bay, Alaska.

| Sample ID (depth interval in cm) | Laboratory number ^a | Material dated | δ ¹³ C (‰) | Lab-reported age (¹⁴ C yr B.P.) | Calibrated age ^b | | Modeled age ^c (2σ cal yr B.P.) |
|---------------------------------------|--------------------------------|----------------------------------|-----------------------|--|-----------------------------|----------------|--|
| | | | | | 1σ cal yr B.P. | 2σ cal yr B.P. | |
| Quicksand Cove (this study) | | | | | | | |
| KEN12-QS7 (47.5–48.3) | OS-103767 | ~8 herbaceous seeds | –26.45 | 185 ± 25 | 284–0 | 295–0 | nd |
| KEN12-QS7 (59.8–60.5) | OS-103784 | Two small twigs | –26.94 | 160 ± 20 | 277–9 | 285–0 | nd |
| KEN12-QS8 (30.7–31.7) | OS-103768 | Two seeds | –24.74 | 240 ± 25 | 304–156 | 422–0 | nd |
| Verdant Cove (Mann and Crowell, 1996) | | | | | | | |
| Deep-out | Beta-74353 | Outer 2 cm of <i>Picea</i> stump | –26.6 | 780 ± 60 | 758–668 | 900–567 | 899–659 |
| B50 | Beta-65022 | Outer 2 cm of <i>Picea</i> stump | –27.3 | 810 ± 50 | 763–683 | 900–666 | 899–671 |
| West outer | Beta-65024 | Outer 2 cm of <i>Picea</i> stump | –28.8 | 940 ± 80 | 930–781 | 981–690 | 957–704 |
| Outer middle | Beta-67121 | Outer 2 cm of <i>Picea</i> stump | –28.9 | 890 ± 70 | 906–735 | 927–691 | 922–697 |
| West pit No. 2 | Beta-67123 | <i>Tsuga</i> , bark on root | –28.6 | 920 ± 50 | 911–790 | 928–736 | 925–735 |
| West pit No. 3 | Beta-67124 | Outer 2 cm of <i>Tsuga</i> stump | –28.9 | 900 ± 50 | 906–761 | 926–727 | 924–726 |
| On bench | Beta-77858 | Peat and wood fragments | –27.4 | 690 ± 60 | 687–562 | 727–550 | 684–546 |
| Under tree | Beta-65023 | Wood | –27.2 | 600 ± 60 | 649–545 | 667–527 | 660–524 |

^a Accelerator mass spectrometry radiocarbon analyses performed at: OS, National Ocean Sciences Accelerator Mass Spectrometry Facility (NOSAMS) at Woods Hole Oceanographic Institution, Woods Hole, Massachusetts; and Beta, Beta Analytic, Inc., Miami, Florida.

^b Radiocarbon ages were calibrated using the computer program Oxcal v4.2.3 (Bronk Ramsey, 2013) with the IntCal13 atmospheric calibration curve (Reimer et al., 2013).

^c Modeled ages performed using Oxcal v4.2.3 (see text for details). Ages from Quicksand Cove not modeled (nd, not determined).

progradation of sand by longshore transport. However, only in the case of the youngest strand plain are closely spaced, north-trending, subtle, low relief (<1 m high), progradational beach ridges apparent on the imagery in Fig. 2. These low relief beach ridges trend obliquely to the frontal 1- to 3-m-high beach ridge, and reflect successive westward progradation of the coastal plain away from the headland. The landward edge of each of the two younger beach ridge sets backs against the escarpment of the next oldest beach ridge set and the oldest beach ridge set backs against the upland (Fig. 2). The two older beach ridge sets each have an undrained depression along part of their landward, southeast edge; and in the case of the landward most beach ridge set, the backedge is, in part, below modern sea level because a tidal pond occurs at the strand plain-to-upland transition (Fig. 2).

The modern beach and the oceanward most beach ridge at Verdant Cove both show evidence of the coastal response to the approximately 1.4 m of subsidence that occurred in the vicinity of Verdant Cove as a consequence of the 1964 earthquake (Plafker, 1969) (Figs. 1B and 4). Because the coast subsided, the seaward-most, pre-1964 beach ridge became more vulnerable to wave attack and erosion.

Through re-deposition of the eroded pre-1964 beach ridge sediment, the post-1964-earthquake beach ridge has formed landward of, and at a higher elevation than, the pre-1964-earthquake beach ridge (Fig. 4). Evidence that the pre-1964-earthquake beach ridge is now partially submerged and eroded is that trees alive in 1964 are now stumps in surf zone and that standing dead, partially buried, trees, alive in 1964, are now

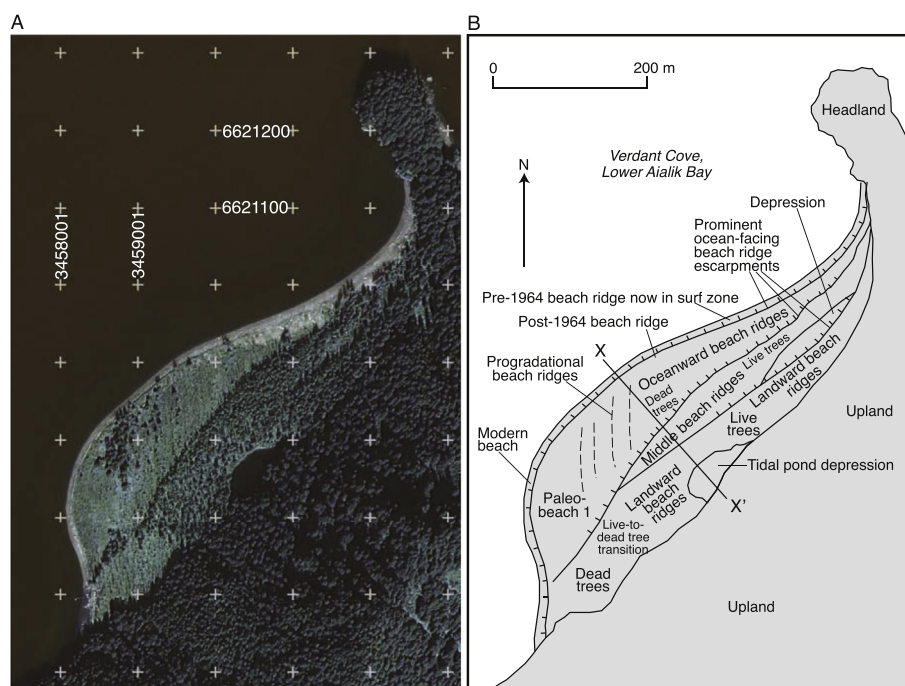


Fig. 2. A. Image of Verdant Cove. Image courtesy of the U. S. National Park Service. Source: IKONOS imagery © GeoEye, all rights reserved. Date of image: August 8, 2005. B. Interpretive line drawing of geomorphic features at Verdant Cove. The Verdant Cove coastal plain is composed of three sets of beach ridges deposited through longshore drift southwestward around the headland.

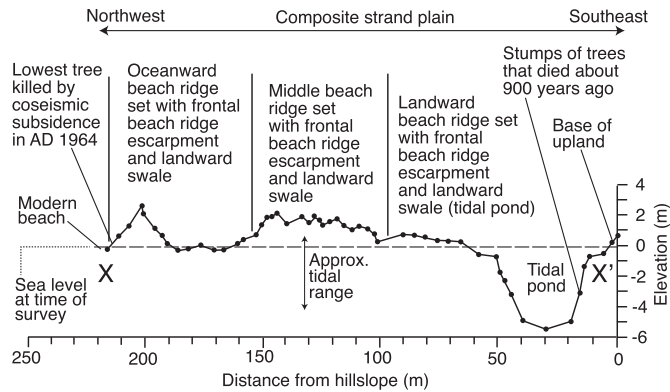


Fig. 3. Topographic profile X–X' on the Verdant Cove coastal plain. See Fig. 2 for location of profile. Level (topographic) data, tidal levels, and data on tree death in A. D. 1964 and 900 years ago reproduced from Mann and Crowell (1996); all other annotations are interpretations added by the authors.

sticking out both on the seaward edge of the modern active beach ridge and also on the backside of the modern beach ridge (Fig. 4). The post-1964 beach ridge is approximately 5 m high above mean tide level, and the crest is actively aggrading because waves are moving cobble and small boulders onto and over the crest of the beach ridge burying standing dead Spruce trees and Spruce trunks on the immediate backside of the beach ridge (Fig. 4). New trees are colonizing the higher parts of the post-1964 beach ridge.

The post-1964 active beach ridge is a compound feature because coseismic subsidence caused erosion of the pre-earthquake beach ridge and subsequent construction of a new beach ridge at a higher elevation and in part on top of the older pre-earthquake beach ridge. The steep escarpment and associated new, higher beach ridge effectively isolated the strand plain to landward and has set the stage for future progradation of a new set of beach ridges to seaward.

4.3. Quicksand Cove

Quicksand Cove is at the downstream end of a drowned glacially-cut valley (Fig. 1C), and a 700-m-long, north-trending beach separates the cove from the Quicksand lowland to the west (Fig. 5). The catchment that drains to Quicksand Cove is underlain by granitic rocks (Wilson and Hults, 2007), and the alluvium in the cove's streams and on the beach is a salt-and-pepper granitic sand with feldspar, quartz and mafic grains that are almost exclusively biotite.

The modern beach at Quicksand Cove is east of two forested relict beach ridges (Fig. 5); each beach ridge has a local relief of 1.6 m (Fig. 6). The youngest relict beach ridge is the highest, and the next youngest (next further inland) is 1.4 m lower. An extensive marsh occurs inland of the next-to-youngest relict beach ridge. The marsh is not flat but has subdued relief (Figs. 5 and 6).

The stratigraphy at Quicksand Cove, depicted at 12 localities through a combination of cores and cutbank exposures (Figs. 5 and 6), includes sand, peat, and silt with lesser components of muddy peat and sandy silt. Most cores bottom out in sand or gravelly sand. The two beach ridges are underlain by sand whereas the marsh stratigraphy in the upper meter below the ground surface is silt and muddy silt with layers of 10–20 cm thick sand (Fig. 6). Stratigraphic units within the upper meter can be correlated among cores and exposures using buried peat or the base of sand units as the basis for correlation (Fig. 6).

The cores and bank exposures cumulatively show three instances of soil burial by inorganic deposits, mainly sand. At the three easternmost core sites, which are on the two emergent, forested relict beach ridges, pits expose sand that buries peaty soils (QS-1, -3 and -10, Fig. 6).

Three radiocarbon age determinations on detrital material contained in the upper cm of the penultimate buried soil (Table 1, Fig. 6B) all indicate that the soil was buried sometime within the last 420 years because the sample ages fall within the pre-AD 1950 plateau of the radiocarbon calibration curve, which extends back to 400 years before AD 1950.

The minimum age of the penultimate buried soil can also be obtained from ^{137}Cs and ^{210}Pb profiles and further limited by the Russian history in the Kenai region. Peak concentration of ^{137}Cs in samples from cores QS-3 and QS-8 overlie the penultimate buried soil and underlie a sand in both cores (Fig. 7); this sand must be younger than 1963, which is the peak of ^{137}Cs concentration in the atmosphere. The absence of ^{137}Cs activity in the penultimate buried soil (Fig. 7) further limits its age to before AD 1950, that is, pre-atomic bomb testing. Historical information, discussed below, provides additional constraints on the minimum age of the penultimate soil.

5. Discussion

5.1. Verdant Cove

The subsidence of the Verdant Cove coastal plain in 1964 instigated an episode of erosion of the seaward-most beach ridge resulting in the formation of a steep, ocean-fronting escarpment (Fig. 4). Such coseismic-subsidence-induced formation of a beach ridge scarp is identical to the process illustrated by Meyers et al. (1996) for beach ridge escarpments formed by coseismic subsidence on the Cascadia subduction zone margin near Willapa Bay, Washington. Using ground-penetrating radar, Meyers et al. (1996) imaged a succession of coastal-parallel, ocean-fronting, buried beach ridge scarps with each scarp subsequently abandoned as the coast prograded seaward during interseismic intervals.

The 1964 coseismic subsidence at Verdant Cove caused a beach escarpment to form because higher relative sea level eroded the pre-earthquake beach and built up, through wave swash, a beach ridge crest at higher elevation (Fig. 4). Coseismic subsidence also caused saline water to intrude the youngest emergent strand plain, weakening and eventually killing the Sitka spruce trees that had colonized the plain (Fig. 2). We anticipate that in the ongoing interseismic interval after the 1964 earthquake, the steep post-1964 escarpment will be preserved by westward progradation of a new strand plain, similar to the penultimate beach ridge escarpment that was preserved by progradation of the oceanward strand set of beach ridges (Fig. 8). This process also is similar to what repeatedly happens on the Long Beach Peninsula near Willapa Bay, Washington, following repeated Cascadia subduction zone earthquakes (Meyers et al. 1996).

We infer that the origin of the two older, paleo beach-ridge escarpments, which are at the seaward edge of the 'middle' and 'landward' beach ridge sets respectively (Figs. 2 and 3), is the product of a similar process of coseismic subsidence followed by formation of an erosional escarpment and build-up of a new, higher beach ridge crest by wave-swash-induced sediment transport and deposition. And the strand plains landward of these escarpments are the result of progradation of beach ridges in the centuries prior to the subsidence that caused the formation of the escarpments. Thus the steep coast-facing escarpment of the highest ridge of a beach ridge set is the signature of a subduction zone earthquake,

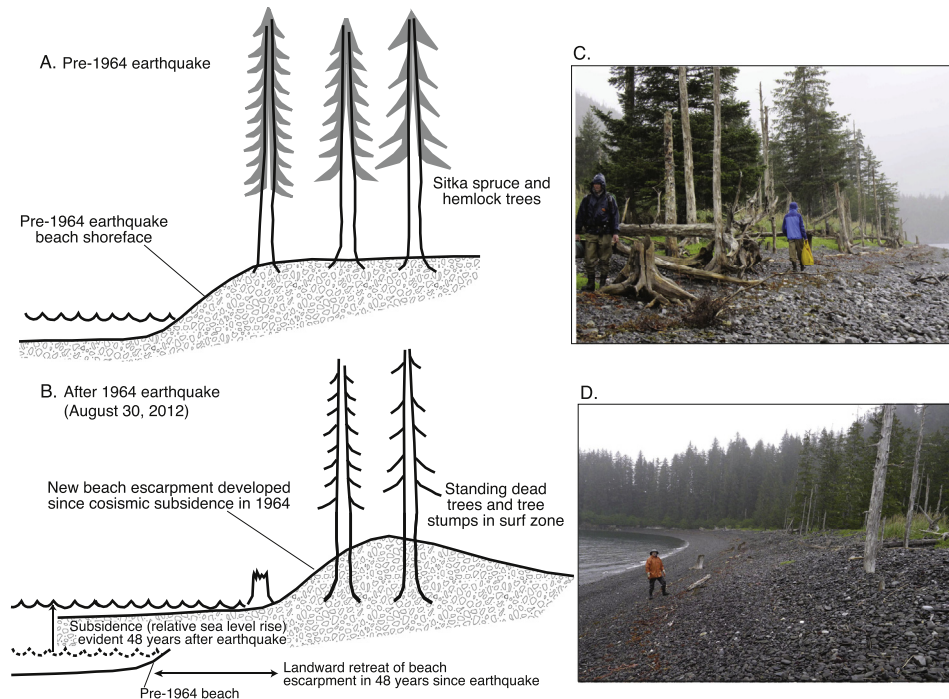


Fig. 4. A. Schematic of pre-1964 beach configuration, Verdant Cove. B. Schematic depiction of beach erosional response at Verdant Cove to co-seismic subsidence during the 1964 subduction zone earthquake. As a consequence of co-seismically lowering of the coast, the beach escarpment erosionally retreated landward and the new beach ridge aggraded in the succeeding years and decades. The modern beach escarpment is approximately 1.5 m high and is caused by landward retreat of the eastern edge of the coastal plain in the 48 years since the earthquake. C. View to southeast down axis of modern beach ridge showing dead Sitka spruce trees killed in response to relative sea level rise and landward retreat of active beach ridge following coseismic subsidence in 1964. The in-place rooted stumps mark the position of the beach ridge prior to the earthquake. D. View to northwest showing new beach escarpment created as a result of coseismic subsidence followed by landward retreat in the years after the 1964 earthquake. Note rooted stump in surf zone marking the pre-1964 earthquake position of the surface of the beach ridge.

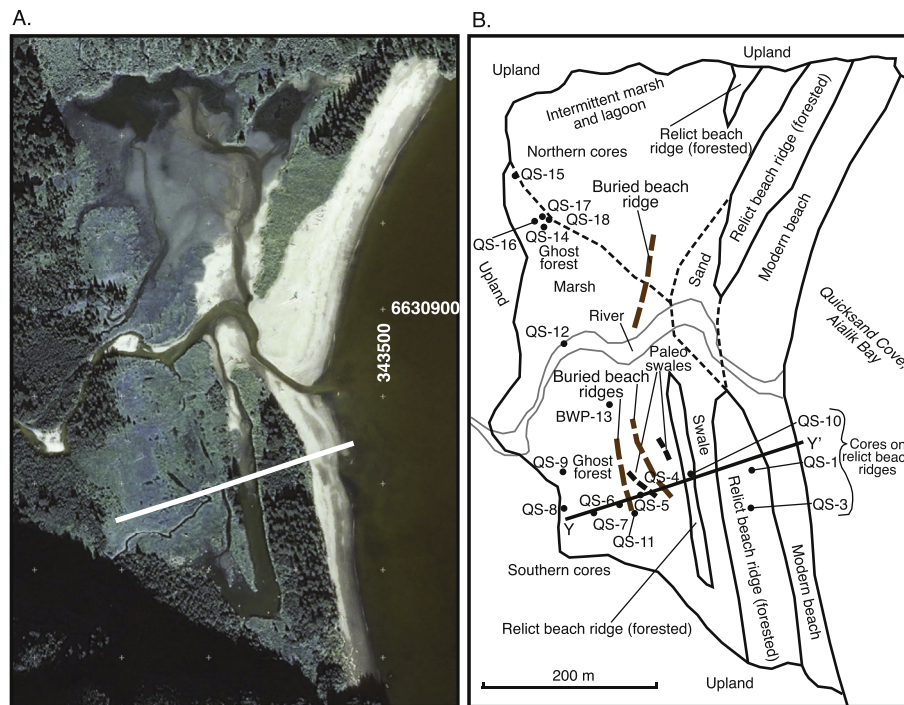


Fig. 5. A. Image of Quicksand Cove. Image courtesy of the U. S. National Park Service. Source: IKONOS imagery © GeoEye, all rights reserved. Date of image: August 8, 2005. B. Interpretive line drawing of geomorphic features at Quicksand Cove. Black dots mark locations of stratigraphic descriptions and samples. For core QS-14, silt at the 6–7 cm depth interval is devoid of foraminifera.

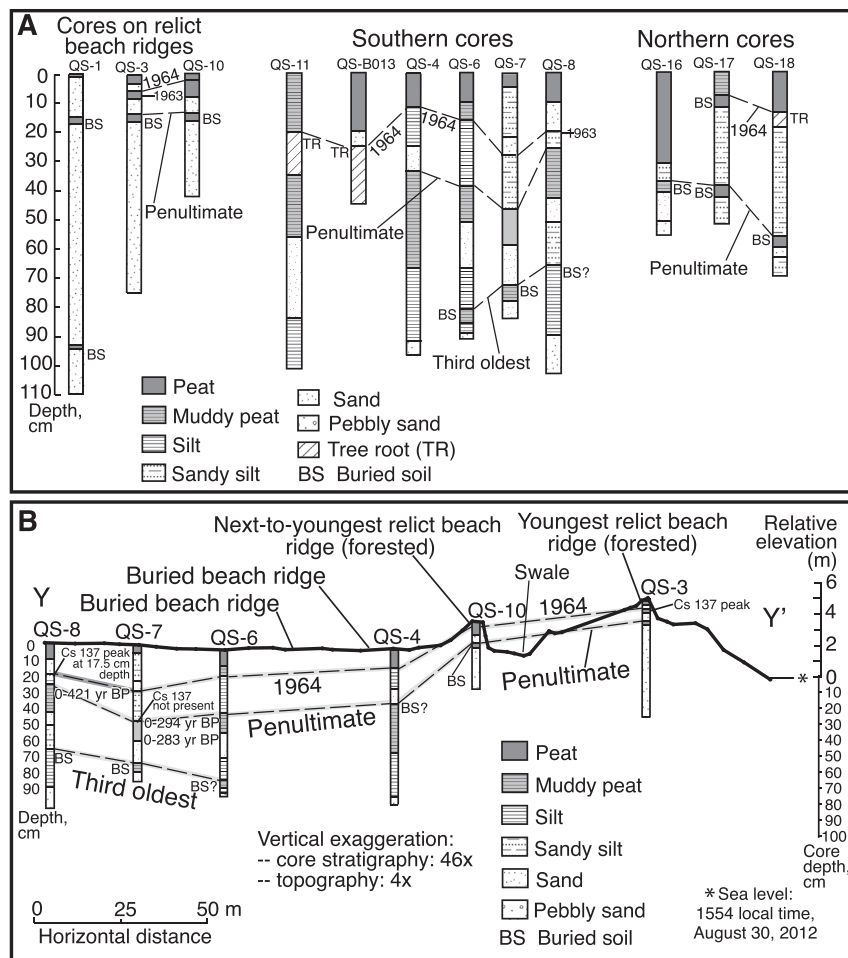


Fig. 6. A. Stratigraphy for 12 cores from Quicksand Cove, divided into three groups of cores based on localized area within the Quicksand Cove lowland. See Fig. 5 for core locations on coastal lowland. "1964" means the 1964 subduction zone earthquake. "Penultimate" means the next-to-youngest subduction zone earthquake. B. Topographic profile Y–Y' across the Quicksand Cove progradational plain surveyed with a real-time kinematic (RTK) global positioning system unit showing selected core stratigraphy that is also depicted above. Location of profile Y–Y' delineated on Fig. 5. The profile shows that the youngest and next-to-youngest forested beach ridge each has a local relief of 1.6 m, with the landward beach ridge 1.4 m lower than the seaward beach ridge.

and the strand plain landward of the escarpment formed in the centuries leading up to that earthquake.

The process of formation of the two older beach ridge escarpments is identical to the process, chronicled above in Section 4.2, for the formation of the modern beach ridge escarpment as a consequence of coseismic subsidence in December 1964. Evidence for sudden submergence associated with formation of the older beach ridge escarpments is dead trees now below sea level on former strand plains fronted by the paleo escarpments. For instance, the trees fringing the tidal pond at the landward edge of the oldest beach ridge set (Figs. 2 and 3) were buried and killed in growth position suggesting submergence was sudden (Mann and Crowell, 1996). Because the Verdant Cove coastal plain has three beach ridge escarpments at the seaward edge of an associated strand plain, we infer the Verdant Cove composite strand plain records relative sea-level changes associated with three subduction zone earthquakes, the AD 1964 earthquake and two, pre-AD 1964, subduction zone earthquakes ('Penultimate' and 'Third oldest', in Fig. 8). And at Verdant Cove, the observation that the beach ridge and associated ocean-facing escarpment gets higher in a coastward direction (Fig. 3) is consistent with gradual relative sea-level rise over multiple subduction zone earthquake cycles.

5.2. Quicksand Cove

In the marsh landward of the two relict forested beach ridges, three submergence events are recorded in both cores and cutbank exposures (Fig. 6). The youngest submergence event is recorded by standing dead forests on the marsh surface (Fig. 5) and by buried, in-place dead roots or buried soils at multiple core sites (Fig. 6). The buried roots of standing dead trees are a proxy for the uppermost buried soil. Based on peak concentrations of ^{137}Cs in two cores in the uppermost buried soil (Fig. 7), the youngest submergence event is most likely the subsidence chronicled along the outer Kenai coast as a consequence of the 1964 earthquake (Plafker, 1969). Therefore, we infer that the 3-to-15-cm-thick sand overlying the youngest buried soil on the seaward-most beach ridge (Fig. 6) is likely a deposit from the 1964 tsunami or deposition as a consequence of post-earthquake-subsidence reorganization of the beach.

Another, deeper buried soil is correlative in cores throughout the marsh (Fig. 6). This next oldest buried soil ("Penultimate", Fig. 6) is recorded on both relict forested beach ridges (cores QS-3 and QS-10) and is also well recorded in river cutbank exposures at QS-16, -17 and -18, where the exposures all contained a buried soil at about a half meter depth. The cutbank buried soil is older than the 1964 soil

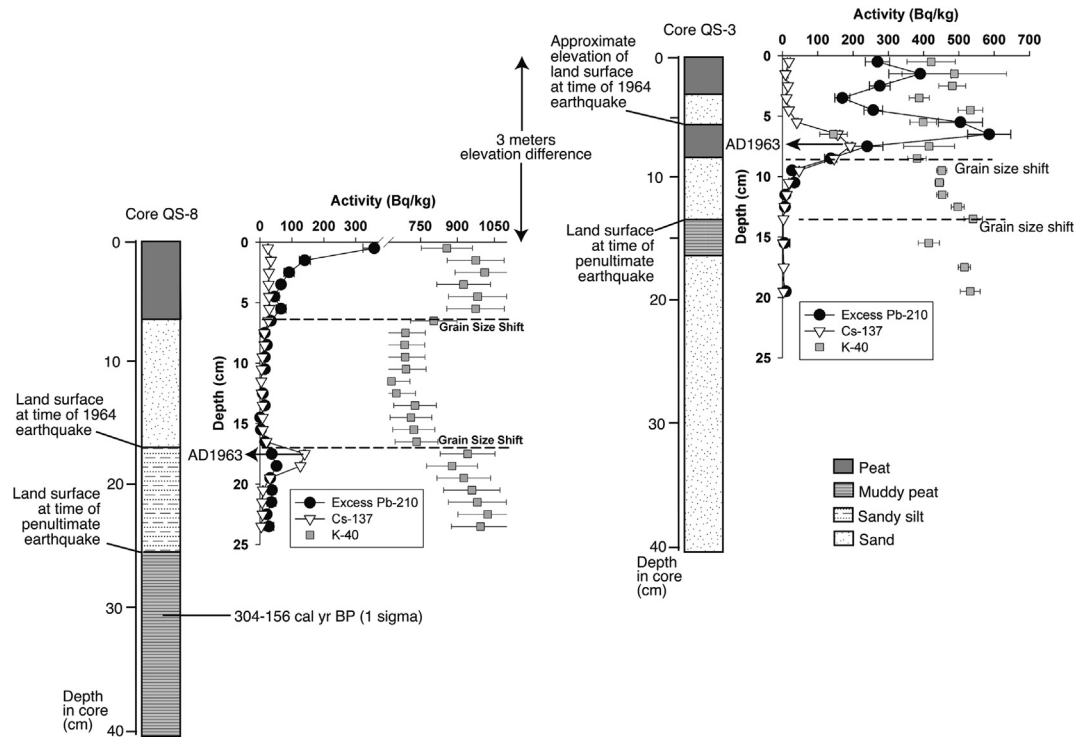


Fig. 7. Downcore ^{210}Pb , ^{137}Cs , and ^{40}K activities for core QS-3 and core QS-8 in comparison to core stratigraphy. For core 8, a significant decrease in ^{40}K activities between 7 and 17 cm is due to the coarser sediments. This same decrease in activity was observed in the excess ^{210}Pb , making an age model calculation difficult. Also for core 8, a distinct peak in ^{137}Cs activity is evident at 18 cm, indicative of 1963 and is followed by a rapid decrease in activity to values at detection limits at ~21 cm. For core 3, a distinct peak in ^{137}Cs activity at 7 cm aids in confirming that the uppermost clean sand is post-1963 and could be a tsunami sand associated with the AD 1964 earthquake.

because trees killed by saline intrusion as a consequence of the 1964 coseismic subsidence were rooted about 35 cm higher than the buried soil exposed in the cutbank (QS-18, Fig. 6).

Because the rupture during the 1964 earthquake caused coseismic subsidence that killed coastal Sitka spruce and hemlock on the Kenai Peninsula (Plafker, 1969), we infer that the next deeper buried soil ('Penultimate', Fig. 6) is also a record of coseismic subsidence and a record of a penultimate earthquake. This penultimate earthquake presumably would have generated a tsunami, and we

infer that clean sand deposited above the second deepest buried soil in a few instances (QS-3, QS-4, QS-10; Fig. 6) is tsunamigenic in origin. But in most cases the second deepest buried soil is not covered by a clean sand deposit because the marsh is protected from direct tsunami incursion by the forested beach ridges to the east. The penultimate buried soil shares three attributes associated with co-seismically buried soils; these attributes include abrupt submergence, a laterally extensive occurrence across the coastal lowland and association with a tsunami (Nelson et al., 1996).

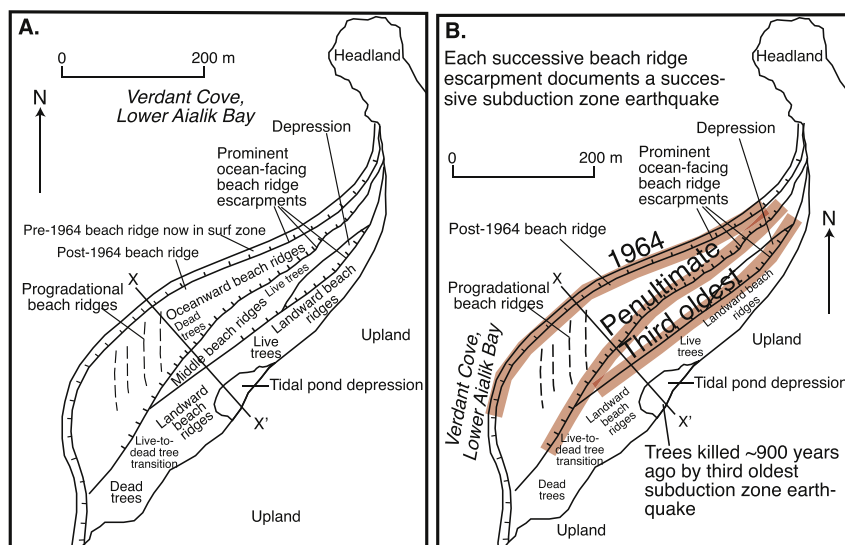


Fig. 8. A. Simplified geomorphic map of Verdant Cove coastal plain B. Interpretation of beach ridge escarpments as chronicles of the last three subduction zone earthquakes.

In Quicksand marsh, there is a third, deeper buried soil observed in three cores in the southern core area (Figs. 5 and 6). We infer a third oldest submergence event based on these observations. The submergence event is not documented throughout the Quicksand marsh and we were unable to identify suitable material to date the time of submergence. The submergence event may have been caused by a subduction zone earthquake about 900 years ago (see discussion below) or may have been caused by a long-lasting closure of a former ocean-fronting, active beach ridge.

5.3. Inferred paleoseismic history on southeast Kenai Coast

Collectively the two sites provide geomorphic and stratigraphic data from which we infer two subduction zone earthquakes older than the 1964 earthquake. In this section, we present constraints on the timing of these two earthquakes and discuss the inferred extents of megathrust rupture.

5.3.1. The third oldest earthquake

Evidence for abrupt submergence at Verdant Cove ca 900 years ago records a third oldest earthquake. This earthquake drowned and killed the trees exposed at the tidal pond (Mann and Crowell, 1966) and caused the formation of the oldest beach ridge escarpment at Verdant Cove.

We used an Oxcal model (Bronk Ramsey, 2009; Lienkaemper and Bronk Ramsey, 2009) to estimate age probability distributions (Fig. 9) for the third oldest earthquake (Earthquake V3 in Fig. 9). Using Mann and Crowell's (1996) maximum and minimum limiting ages yields an estimated range of 590–740 cal yr BP (AD 1360–1210) for earthquake V3 (Fig. 9B). However, the minimum limiting ages used in the Oxcal model provide a poor constraint for the time of earthquake subsidence. Mann and Crowell's (1996)

minimum limiting ages are from detritus in the peat that accumulated in multiple tens to hundreds of years after the trees died, whereas maximum limiting ages, which are on bark or from the outer 2 cm of earthquake-killed trees (Mann and Crowell, 1996), reflect the timing of subsidence to within a decade or less. Therefore, the estimate for the age of the V3 earthquake (Fig. 9C) is too young because the maximum limiting age derived from drowned trees is much closer to the true age than minimum age constraints derived from the overlying peat.

As an alternative, we use earthquake age modeling to test the hypothesis that the Verdant Cove trees were killed by the same ~900 cal yr BP earthquake (i.e., earthquake E1, Fig. 9) that is documented by Shennan et al. (2014a) at the Copper River delta, Katalla and Puffy Slough (locations on Fig. 10). If minimum limiting ages for earthquake E1 are older than the maximum limiting ages used to define Verdant Cove earthquake V3, then the Verdant Cove trees died after the second-to-youngest earthquake that affected Copper River delta, Katalla and Puffy Slough. But if ages for earthquake E1 are not older, then we have not invalidated the hypothesis that the Verdant Cove trees were killed by the same earthquake E1 documented by Shennan et al. (2014a).

The model results indicate that the minimum limiting age for Shennan et al.'s (2014a) earthquake E1 are not older than the maximum limiting ages for earthquake V3 at Verdant Cove. Therefore we can define a hybrid age model V3* (Fig. 9C) for the age of an earthquake in which the older end is constrained by the Verdant Cove stump ages and the younger end is constrained by the younger limiting ages for earthquake E1 in the Copper River delta, Katalla and Puffy Slough coastal areas. The age of the V3* earthquake (Fig. 9C) has a median of 867 cal yr BP (AD 1083) and a 2-sigma range of 840–890 cal yr BP (AD 1110–1060). These ages permit, but do not require, that the Verdant Cove trees were killed

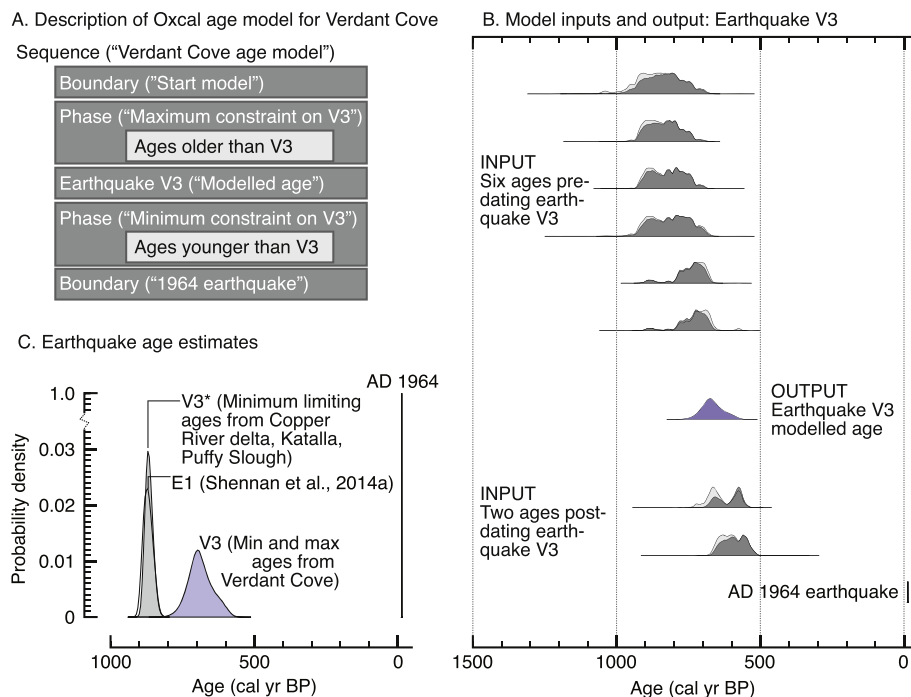


Fig. 9. A. Oxcal model approach to model age of inferred earthquake V3. B. Data used in the model. Light gray pdfs: calibrated ages for each of the Verdant Cove radiocarbon age determinations in Mann and Crowell (1996). Dark gray pdfs: trimmed ages using Oxcal's Bayesian approach given the knowledge that the stump ages are older than earthquake V3 and the peat and decayed wood ages are younger than the earthquake. Purple pdf: statistical probability of the earthquake V3 age, expressed as a pdf, given older and younger limiting ages. C. Age model V3 compared to age model E1 of Shennan et al. (2014a) compared to hybrid age model V1*. The results of the hybrid age model provide a test of the hypothesis that the Verdant Cove tidal pond trees were killed by the same Prince William Sound earthquake that has a model age of E1. See text for further explanation.

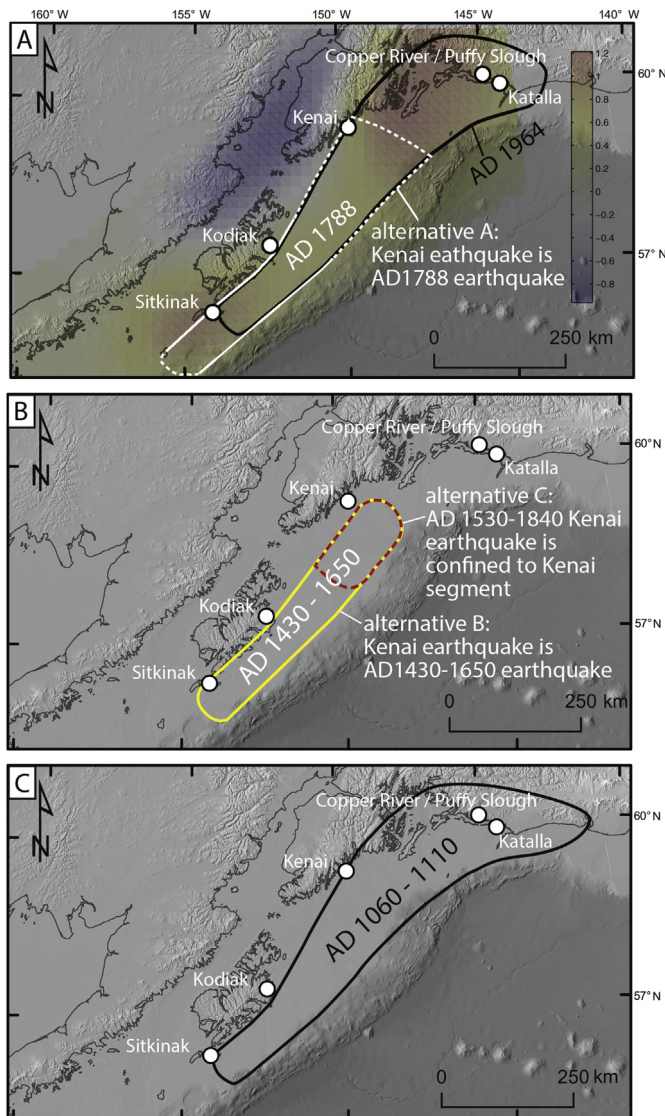


Fig. 10. Three alternatives for the tectonic context of the penultimate AD1530–1840 Kenai earthquake in comparison to the AD 1964 earthquake and the third oldest earthquake. A. Coseismic uplift extent of the AD1964 earthquake on which is superposed the inferred coseismic uplift extent of the AD1788 rupture, if this historic earthquake involved rupture of the Kenai segment (alternative A). The colors show geodetic coupling ratio units as a fraction of the contemporary Pacific–North American plate rate, taken from Zweck et al., 2002. B. Alternative B (yellow) is the inferred uplift extent of the AD 1430–1650 subduction zone earthquake if this earthquake involved rupture of the Kenai segment. Alternative C (red) is the inferred uplift extent of the penultimate Kenai earthquake if earthquake rupture involved the Kenai segment alone. C. Inferred uplift extent for the ~900 cal yr BP earthquake, which is recorded in Prince William Sound, on the Kenai Peninsula (this study) as well as on Kodiak and Sitkinak Islands. Data sources: Briggs et al., 2014; Shennan et al., 2014a; 2014b; 2014c; Shennan, 2009; Shennan et al., 2009; Freymueller et al., 2008; Zweck et al., 2002; Mann and Crowell, 1996; Plafker, 1969.

by the same ~900 cal yr BP earthquake that is documented at the Copper River delta, Katalla and Puffy Slough (earthquake E1, Shennan et al., 2014a) (Fig. 10).

5.3.2. The penultimate Kenai earthquake

The penultimate Kenai earthquake is estimated to have occurred in the age range AD 1530–1840. Based on radiocarbon age determinations (Table 1) and ^{137}Cs analyses (Fig. 7), an abrupt subsidence event at Quicksand Cove, caused by the penultimate earthquake, is pre-1950 and younger than about 420 years before

AD 1950 (i.e., AD 1530). The penultimate earthquake occurs in the age range where the radiocarbon calibration curve is flat and thus calibrated age ranges span four centuries before AD 1950. In southern Alaska, Russian settlement of the Kenai region makes the occurrence of the penultimate earthquake unlikely after about AD 1840. Although not continuous, archival records of the Russian–American Company and the Russian Orthodox Church in Alaska are sufficiently detailed that very strong ground shaking or the occurrence of a damaging tsunami from a great subduction zone earthquake that affected the entire Kenai Peninsula region would probably have been recorded after AD 1840. From AD 1840 onward, there is no mention of shaking, tsunami or coastal elevation change in studied Russian historical accounts from the Kenai Peninsula (Lander, 1996; Black, 2004). Therefore the penultimate earthquake, which produced an erosional beach ridge escarpment at Verdant Cove and occasioned the abrupt burial of soil and trees at Quicksand Cove, is prehistoric (pre-AD 1840) but younger than the older end of the calibration age range (AD 1530).

The AD 1530–1840 Kenai penultimate earthquake overlaps in age with two documented subduction zone earthquakes to the west on Kodiak Island. The age range of the Kenai penultimate earthquake overlaps the age range of a subduction zone earthquake on and near Kodiak Island in AD 1430–1650 as documented by Briggs et al. (2014) on Sitkinak Island and by Shennan et al. (2014c) in numerous sites on Kodiak Island. The Kenai penultimate earthquake also overlaps in age with the AD 1788 subduction zone earthquake documented in Russian accounts. The earthquake of 21 July AD 1788 caused a 3–10 m tsunami that forced relocation of the first Russian settlement at Three Saints Bay on southwestern Kodiak Island (Soloviev, 1990; Lander, 1996; Briggs et al., 2014). Shennan et al. (2014c) describe stratigraphic evidence for land level change on Kodiak Island that they infer to have occurred during the AD 1788 earthquake. Rupture of the Kodiak segment of the megathrust has been inferred to explain both earthquakes (Briggs et al., 2014; Shennan et al., 2014c).

We do not know whether this single earthquake at Kenai in the age range AD 1530–1840 was the AD 1788 historic earthquake, the AD 1430–1640 earthquake of Briggs et al. (2014) and Shennan et al. (2014c), or a different earthquake that occurred at the same general time but was localized to the Kenai segment. In either of the first two scenarios, the extent of ruptures involving the Kodiak segment would be extended to the northeast based on evidence at Quicksand and Verdant coves (Alternatives A and B, Fig. 10). In the third scenario, rupture limited to the Kenai segment alone (Alternative C, Fig. 10) would account for the penultimate Kenai earthquake evidence, and both the AD 1430–1650 earthquake and the AD 1788 earthquakes would reflect rupture of the Kodiak segment and possibly areas further west (Briggs et al., 2014; Shennan et al., 2014c) and not rupture of the Kenai segment.

5.4. Conditions under which beach ridges can be paleoseismic indicators, southeast coast of Kenai Peninsula

Beach ridges previously have been recognized as indicators of coseismic land-level change. Two classic examples of a set of beach ridges documenting coseismic uplift include Cape Turakirae, New Zealand (Aston, 1912; Wellman, 1969; McSaveney et al., 2006; Little et al., 2009) and Isla Mocha offshore of mainland Chile (Nelson and Manley, 1992). For rapid post seismic emergence, the Kiritappu coastal lowland, Hokkaido (Kelsey et al., 2006; Sawai et al., 2009) hosts beach ridges that are inferred to correlate with post-seismic rapid emergence events. And at the Cascadia subduction zones, Meyers et al. (1996) document, as discussed previously, how beach ridge escarpments on the Willapa barrier spit can form as a result of coseismic subsidence. The above sites differ in the type of rapid, or

co-seismic, relative sea-level change; but these sites have in common a high wave energy coast and, at the location of beach ridges, no fluvial sediment input to the coast. Monecke et al. (2014) show that co-seismic subsidence from the 2004 Andaman–Aceh earthquake triggered erosion of the active beach ridge on the south Aceh coast and rebuilding of a new beach ridge in the following few years. But the south Aceh coast is a sediment-supply-rich system, and other mechanisms besides co-seismic subsidence may form, and preserve, beach ridges.

On the southeast coast of the Kenai Peninsula, beach ridges can be excellent indicators of co-seismic subsidence in settings where a prograding strand plain attaches to the leeward side of a headland unindented by a coastal drainage. At Verdant Cove, where beach ridges prograde in front of a steep coast with no indenting drainage mouth, abrupt co-seismic subsidence triggers erosion of the beach ridge and therefore formation of beach ridge erosional escarpments that may correlate one-to-one with co-seismic land level changes (Fig. 8B).

In contrast, embayments at the mouths of streams, such as Quicksand Cove, can form aggrading coastal lowlands amenable to coring investigations and thus can chronicle co-seismic subsidence. But embayments are a setting where beach ridge formation is less easily isolated to a single cause. In embayments, two additional processes that may contribute to beach ridge formation or burial are barrier bar closures and sediment mobilization within embayments during times of floods from upstream basins. Despite these complicating factors, Quicksand Cove has two forested beach ridges with ocean-fronting erosional escarpments. We infer that these escarpments document co-seismic subsidence during subduction zone earthquakes. However, without the observations at Verdant Cove, these candidate co-seismic erosion scarps may not have been identified.

6. Implications for megathrust rupture and seismic hazard

Similar to the AD 1964 great Alaska earthquake, an earthquake in the interval AD 1060–1110 may have ruptured the Kodiak, Kenai and Prince William Sound segments of the subduction zone (Fig. 10) based on inferred co-seismically buried soils or buried trees in all three regions that have overlapping age ranges (e.g., Mann and Crowell, 1996; Shennan, 2009; Shennan et al., 2009).

But the AD 1530–1840 Kenai penultimate earthquake on the southeast Kenai coast did not rupture northeastward to Prince William Sound. As discussed above, there are three alternatives for the timing and extent of the Kenai penultimate earthquake (Fig. 10). Each of the three alternatives lead to the same two major conclusions. First, ruptures have extended across or occurred within parts of the Alaska–Aleutian megathrust that currently show variable locking/creeping behavior (e.g., Fig. 1). Second, the Kenai segment can rupture independently of the Prince William Sound segment. Similar variable behavior has been noted at the southern end of Kodiak Island, where paleoearthquakes have both stopped and ruptured through the southwestern end of the 1964 rupture (Briggs et al., 2014). Thus eastern Alaska–Aleutian subduction zone earthquakes can both propagate through multiple segments with varying degrees of coupling, as is the case with both the AD 1964 and the 900-year-ago subduction zone earthquakes, but also stop near the edges of apparently more highly-coupled patches, as appears to be the case for the penultimate Kenai earthquake that did not rupture the Prince William Sound segment.

The seismic hazard implication of the above observation for Alaska is that partially locked subduction zone segments that are presently creeping have ruptured in conjunction with neighboring locked segments in the past and have ruptured while neighboring segments remain locked. And, in Alaska, historically observed slip

patches correspond with areas that appear to be locked presently based on geodetic observations. But we show that these presently locked areas do not necessarily rupture in all past earthquakes. This result suggests caution be used when employing historically observed slip patches (Ichinose et al., 2007; Freymueller et al., 2008) and geodetic locking models (Zweck et al., 2002) to infer future hazard.

Acknowledgments

Coastal site investigations were carried out utilizing the U.S. Geological Survey's research vessel Alaskan Gyre under the capable command of Captain Greg Snegden. The National Park Service provided access to the two sites, which are both within Kenai Fjords National Park. Boat operation, USGS staff, and radiocarbon age determinations were supported by the U. S. Geological Survey's Earthquake Hazards Program. Keith Labay provided assistance with map-based graphics. We thank Torbjörn Törnqvist, Ian Shennan, and two anonymous reviewers for helpful reviews. Manuscript was prepared while Kelsey was a Visiting Scholar in the Department of Earth and Space Sciences at the University of Washington.

References

- Aston, B.C., 1912. The raised beaches of Cape Turakirae. *Trans. Proc. N. Z. Inst.* 44, 208–213.
- Black, L.T., 2004. *Russians in Alaska: 1732–1867*. University of Alaska Press, p. 344.
- Briggs, R.W., Engelhart, S.E., Nelson, A.R., Dura, T., Kemp, A.C., Haeussler, P.J., Corbett, D.R., Angster, S.J., Bradley, L.A., 2014. Uplift and subsidence reveal a nonpersistent megathrust rupture boundary (Sitkinak Island, Alaska). *Geophys. Res. Lett.* 41, 2289–2296. <http://dx.doi.org/10.1002/2014GL059380>.
- Bronk Ramsey, C., 2009. Bayesian analysis of radiocarbon dates. *Radiocarbon* 51, 337–360.
- Bronk Ramsey, C., 2013. OxCal 4.2.2 Manual. <https://c14.arch.ox.ac.uk>.
- Cable, J., Burnett, W., Moreland, S., Westmoreland, J., 2001. Empirical assessment of gamma ray self-absorption in environmental analyses. *Radioact. Radiochem.* 12, 30–39.
- Carver and Plafker, 2008. Paleoseismicity and neotectonics of the Aleutian subduction zone – an overview. In: Freymueller, J.T., Haeussler, P.J., Wesson, R.L., Ekstrom, G. (Eds.), *Active Tectonics and Seismic Potential of Alaska*, Geophysical Monograph 179 American Geophysical Union, Washington, D.C., pp. 43–63.
- Christensen, D.H., Beck, S.L., 1994. The rupture process and tectonic implications of the great 1964 Prince William Sound earthquake. *Pageoph* 142, 29–53.
- Cutshall, N.H., Larsen, I.L., Olsen, C.R., 1983. Direct analysis of ^{210}Pb in sediment samples: self-absorption corrections. *Nucl. Instrum. Methods* 206, 309–312.
- Freymueller, J.T., et al., 2008. Active deformation processes in Alaska, based on 15 years of GPS measurements. In: Freymueller, J.T., Haeussler, P.J., Wesson, R.L., Ekstrom, G. (Eds.), *Active Tectonics and Seismic Potential of Alaska*, Geophysical Monograph 179 American Geophysical Union, Washington, D.C., pp. 1–42.
- Goy, J.L., Zazo, C., Dabrio, C.J., 2003. A beach-ridge progradational complex reflecting periodical sea-level and climate variability during the Holocene, Gulf of Almeria, western Mediterranean. *Geomorphology* 50, 251–268.
- Hein, C.J., Fitzgerald, D.M., Cleary, W.J., Albernaz, M.B., De Menezes, J., Klein, A., 2013. Evidence for a transgressive barrier within a regressive strandplain system: implications for complex coastal response to environmental change. *Sedimentology* 60, 469–502. <http://dx.doi.org/10.1111/j.1365-3091.2012.01348.x>.
- Ichinose, G., Somerville, P., Thio, H.K., Graves, R., O'Connell, D., 2007. Rupture process of the 1964 Prince William Sound, Alaska, earthquake from the combined inversion of seismic, tsunami, and geodetic data. *J. Geophys. Res.* 112, B07306. <http://dx.doi.org/10.1029/2006JB004728>.
- Kelsey, H.M., Satake, K., Sawai, Y., Sherrod, B., Shimokawa, K., Shishikura, M., 2006. Recurrence of post seismic coastal uplift, Kurile subduction zone, Japan. *Geophys. Res. Lett.* 33 <http://dx.doi.org/10.1029/2006GL026052>.
- Lander, J.F., 1996. *Tsunamis Affecting Alaska 1737–1996*. NOAA/NGDC, Boulder, CO, p. 195.
- Lienkaemper, J.J., Bronk Ramsey, C., 2009. OxCal: versatile tool for developing paleoearthquake chronologies – a primer. *Seismol. Res. Lett.* 80, 431–434.
- Little, T.A., Van Dissen, R., Schermer, E., Carne, R., 2009. Late Holocene surface ruptures on the southern Wairarapa fault, New Zealand: link between earthquakes and the uplifting of beach ridges on a rocky coast. *Lithosphere* 1, 4–28.
- Mann, D.H., Crowell, A.L., 1996. A large earthquake occurring 700–800 years ago in Aialik Bay, southern coastal Alaska. *Can. J. Earth Sci.* 33, 117–126.
- McSaveney, M.J., Graham, I., Begg, J., Beau, A., Hull, A., Kim, K., Zondervan, A., 2006. Late Holocene uplift of beach ridges at Turakirae Head, south Wellington coast, New Zealand. *N. Z. J. Geol. Geophys.* 49, 337–358.

- Meyers, R.A., Smith, D.G., Jol, H.M., Peterson, C.D., 1996. Evidence for eight great earthquake-subsidence events detected with ground-penetrating radar, Willapa barrier, Washington. *Geology* 24, 99–102.
- Monecke, K., 14 others, 2014. Beach ridge patterns in West Aceh, Indonesia, and their response to large earthquakes along the northern Sunda trench. *Quat. Sci. Rev.* <http://dx.doi.org/10.1016/j.quascirev.2014.10.014> in press.
- Nelson, A.R., Manley, W.F., 1992. Holocene coseismic and aseismic uplift of Isla Mocha, south-central Chile. *Quat. Int.* 15/16, 61–76.
- Nelson, A.R., Shennan, I., Long, A.J., 1996. Identifying coseismic subsidence in tidal-wetland stratigraphic sequences at the Cascadia subduction zone of western North America. *J. Geophys. Res.* 101, 6115–6135.
- Otvos, E.G., 2000. Beach ridges – definitions and significance. *Geomorphology* 32, 83–108.
- Plafker, G., 1969. Tectonics of the March 27, 1964, Alaska Earthquake. *US Geological Survey Professional Paper*, 543-I, p. 74.
- Reimer, P.J., Bard, E., Bayliss, A., Beck, J.W., Blackwell, P.G., Bronk Ramsey, C., Buck, C.E., Cheng, H., Edwards, R.L., Friedrich, M., Grootes, P.M., Guilderson, T.P., Hafflason, H., Hajdas, I., Hatt, C., Heaton, T.J., Hogg, A.G., Hughen, K.A., Kaiser, K.F., Kromer, B., Manning, S.W., Niu, M., Reimer, R.W., Richards, D.A., Scott, E.M., Southon, J.R., Turney, C.S.M., van der Plicht, J., 2013. IntCal13 and MARINE13 radiocarbon age calibration curves 0–50,000 years cal BP. *Radio-carbon* 55, 1869–1887. http://dx.doi.org/10.2458/azu_js_rc.55.16947.
- Sawai, Y., Kamataki, T., Shishikura, M., Nsai, H., Okamura, Y., Satake, K., Thomson, K.H., Matsumoto, D., Fujii, Y., Komatsubara, J., Aung, T.T., 2009. Aperiodic recurrence of geologically recorded tsunamis during the past 5500 years in eastern Hokkaido, Japan. *J. Geophys. Res.* 114 <http://dx.doi.org/10.1029/2007JB005503>.
- Shennan, I., 2009. Late Quaternary sea-level changes and palaeoseismology of the Bering Glacier region, Alaska. *Quat. Sci. Rev.* 28, 1762–1773. <http://dx.doi.org/10.1016/j.quascirev.2009.02.006>.
- Shennan, I., Bruhn, R., Plafker, G., 2009. Multi-segment earthquakes and tsunami potential of the Aleutian megathrust. *Quat. Sci. Rev.* 28, 7–13. <http://dx.doi.org/10.1016/j.quascirev.2008.09.016>.
- Shennan, I., Bruhn, R., Barlow, N., Good, K., Hocking, E., 2014a. Late Holocene great earthquakes in the eastern part of the Aleutian megathrust. *Quat. Sci. Rev.* 84, 86–97.
- Shennan, I., Barlow, N., Combellick, R., Pierre, K., Stuart-Taylor, O., 2014b. Late Holocene paleoseismology of a site in the region of maximum subsidence during the 1964 Mw 9.2 Alaska earthquake. *J. Quat. Sci.* ISSN: 0267-8179 <http://dx.doi.org/10.1002/jqs.2705>.
- Shennan, I., Barlow, N., Carver, G., Davies, F., Garrett, E., Hocking, E., 2014c. Great tsunamigenic earthquakes during the past 1000 yr on the Alaska megathrust. *Geology* 42, 687–690.
- Soloviev, S.L., 1990. Sanak-Kodiak tsunami of 1788. *Sci. Tsunami Hazards* 8, 34–38.
- Suito, H., Freymueller, J.T., 2009. A viscoelastic and afterslip postseismic deformation model for the 1964 Alaska earthquake. *J. Geophys. Res.* 114, B11404. <http://dx.doi.org/10.1029/2008JB005954>.
- Wellman, H.W., 1969. Tilted marine beach ridges at Cape Turakirae, New Zealand. *Tuatara* 17, 82–93.
- Wells, L.E., 1996. The Santa Beach ridge complex: sea-level and progradational history of an open gravel coast in central Peru. *J. Coast. Res.* 12, 1–17.
- Wilson, F.H., Huels, C.P., 2007. compilers, *Geology of the Prince William Sound and Kenai Peninsula Region, Alaska*. U. S. Geological Survey, Dept. of the Interior, Scientific Investigations Map.
- Witter, R.C., Kelsey, H.M., Hemphill-Haley, E., 2003. Great Cascadia earthquakes and tsunamis of the past 6,700 years, Coquille River estuary, southern coastal Oregon. *Geol. Soc. Am. Bull.* 115, 1289–1306.
- Zweck, C., Freymueller, J.T., Cohen, S.C., 2002. Three-dimensional elastic dislocation modeling of the postseismic response to the 1964 Alaska earthquake. *J. Geophys. Res.* 107 (B4) <http://dx.doi.org/10.1029/2001JB000409>.